Mutation of R116C results in highly oligomerized alpha A-crystallin with modified structure and defective chaperone-like function

ARTICLE *in* BIOCHEMISTRY · MARCH 2000

Impact Factor: 3.02 · Source: PubMed

4 AUTHORS, INCLUDING:

Sibes Bera
Saint Louis University
25 PUBLICATIONS **528** CITATIONS

SEE PROFILE

Mutation of R116C Results in Highly Oligomerized αA-Crystallin with Modified Structure and Defective Chaperone-like Function†

Nilufer P. Shroff, Mary Cherian-Shaw, Sibes Bera, and Edathara C. Abraham*

Department of Biochemistry and Molecular Biology, Medical College of Georgia, Augusta, Georgia 30912-2100

Received July 19, 1999; Revised Manuscript Received October 6, 1999

ABSTRACT: An autosomal dominant congenital cataract in human is associated with mutation of Arg-116 to Cys (R116C) in αA-crystallin. To investigate the molecular basis of cataract formation, rat αA-crystallin cDNA was cloned into pET-23d(+), and the site-directed mutants S142C (similar to wild-type human αA) and R116C/S142C or R116C (similar to human R116C variant) were generated. These were expressed in *E. coli* and the recombinant αA-crystallins purified by Sephacryl size-exclusion chromatography. The chaperone-like function of mutant R116C determined at 37 °C with insulin and alcohol dehydrogenase as target proteins was about 40% lower than those of wild-type and mutant S142C. Based on size-exclusion chromatography data, the oligomeric size of the R116C mutant was about 2000 kDa at 25 °C, 1400 kDa at 37 °C, and 900 kDa at 45 °C. In comparison, αA-wild-type and αA-S142C ranged from 477 to 581 kDa. Heat stability studies corroborated the effect of temperature on the dynamic quaternary structure of the R116C mutant. Circular dichroism spectra showed secondary and tertiary structural changes, and ANS fluorescence spectra showed loss of surface hydrophobicity in the R116C mutant. These findings suggest that the molecular basis for the congenital cataract with the αA-R116C mutation is due to the generation of a highly oligomerized αA-crystallin having a modified structure and decreased chaperone-like function.

α-Crystallin constitutes about 25−50% of the total soluble protein in the lens and is believed to be a major structural element in the highly concentrated protein matrix which is essential for maintenance of transparency. Native α-crystallin is composed of αA- and αB-subunit polypeptides with molecular weights of approximately 20 000 each (*1*, *2*). αA and αB share 57% identity in their polypeptide chains (*1*). The human αA and αB genes have been localized to chromosomes 21 (17 in rat) and 11, respectively (*3*, *4*). αA-Crystallin is expressed extralenticulary in small amounts in the brain, liver, spleen, retina, and thymus (*5*, *6*). αB-Crystallin is most abundant in the lenticular tissue, and is also expressed in cardiac muscle, skeletal muscle, brain, retina, and lung (*7*, *8*). There is involvement of hsps and αB-crystallin in major cytomorphological organization during normal growth and under pathological conditions (*9*−*13*). α-Crystallin oligomers have a molecular mass in the 300−800 kDa range (*14*, *15*). Both subunits of α-crystallin share sequence similarity with small heat-shock protein, and this sequence homology is confined to a stretch of 100 amino acids in the C-terminal domain (*16*). In addition to its structural function, Horwitz (*17*) demonstrated that α-crystallin in vitro has chaperone-like activity, a feature which allows it to suppress aggregation of other proteins. The presence of an active molecular chaperone α-crystallin may be essential for maintaining lens transparency. Brady et al. (*18*) generated a knock-out mouse homologous for the αA-crystallin gene. The αA-crystallin −/− mice had no detectable αA-crystallin in their lens, and the lens size was slightly smaller than the wild-type lenses but had normal gross structure. However, several weeks after birth, lens opacification and dense inclusion bodies that contained insoluble αB-crystallin in the lens fiber cells were seen. This was the first in vivo report showing the necessity of αA-crystallin for maintenance of lens clarity and solubility of αB-crystallin.

Due to its large oligomeric size and its microheterogeneity, the quaternary structure has eluded both NMR and crystallographic studies. Haley et al. (*19*), using cryo-electron microscopy (cryo-EM) and image processing, analyzed the structure of recombinant human αB-crystallin. They proposed that αB-crystallin has an asymmetric quaternary structure with variable monomer binding and it forms roughly spherical particles with a large central cavity and a protein shell which has a lot of structural divergence. The proposed structure of the recombinant αB-crystallin is similar to the crystal structure of a small heat-shock protein from *Methanococcus jannaschii.* It is composed of 24 monomers and assumes a hollow spherical complex with octahedral symmetry having 8 trigonal and 6 square windows (*20*). In αA-crystallin, site-directed spin-label studies of the amino acid residues between 109 and 120 revealed the presence of a β-strand containing the buried residues R112 and R116 (*21*). Further studies demonstrated that residues between 84 and 120 had antiparallel β-sheets consisting of three strands arranged in consecutive β-hairpins (*22*).

Congenital cataracts are a common cause of blindness in infants (*23*). Autosomal dominant congenital cataract is the most common familial form (*24*). Several types of mutations occurring in mammalian crystallin genes are associated with

† This work was supported by Grants EY 11352 and EY 07394 from the National Institutes of Health.

* To whom correspondence should be addressed.

10.1021/bi991656b CCC: $19.00
Published on Web 01/12/2000

hereditary cataracts (*25*−*30*). An autosomal dominant cataract associated with a missense mutation in the human αA-crystallin gene has been reported recently (*30*). In this form of cataract, the αA-crystallin mutation Arg-116 to Cys (R116C) was observed. However, it has not been shown how this mutation in αA-crystallin leads to cataract in the affected persons and whether this mutation causes structural and functional changes in αA-crystallin. Rat αA-crystallin has 98% sequence homology with human αA-crystallin, and residues 109−120 show 100% homology. Due to this strong sequence homology and since it is difficult to obtain a human αA-crystallin clone, we have cloned rat αA-crystallin and generated a rat αA-crystallin containing the same mutation. This study demonstrates that the mutant R116C exists as a highly oligomerized protein with perturbed secondary and tertiary structures and decreased chaperone-like activity.

EXPERIMENTAL PROCEDURES

Cloning and Site-Directed Mutagenesis of Rat αA-Crystallin DNA. Total RNA was isolated using Trizol Reagent (Life Technologies) from a 1-month-old fresh rat lens. RT-PCR was done using the upstream primer 5′-CCC AAG CTT TCA GGA AGG CAG ACT CTT T-3′ containing an *Eco*RV site and the downstream primer 5′-CCC GAT ATC ATG GAC GTC ACC ATC CA-3′ containing a *Hin*dIII site. The αA-crystallin DNA was ligated into *Eco*RV-digested pGEM-T vector (Promega) and used to transform DH5α *E. coli* cells (Stratagene). Plasmid DNA from the resulting clones was sequenced by automated DNA sequencing (ABI Prism 377 DNA sequencer). To subclone into the expression vector, pET-23d(+) (Novagen) was sequentially digested with *Nco*I, mung bean nuclease, and *Hin*dIII, and the αA-crystallin DNA was excised from pGEM-T using *Hin*dIII and *Eco*RV and ligated into this vector. The QuickChange Site-Directed Mutagenesis Kit (Stratagene) was used to generate the mutants αA-S142C and αA-R116C/S142C (abbreviated as R116C), and their nucleotide sequences were confirmed by automated DNA sequencing.

Expression and Purification of Recombinant Wild-Type and Mutant αA-Crystallins. BL21(DE3)pLysS *E. coli* cells (Novagen) were used as the expression host. These cells were transformed with the appropriate amplicons and grown in 500 mL of Luria broth at 37 °C with aeration. At an $OD_{600\ nm} \approx 0.6$, the T7 promoter was induced using 0.5 mM isopropyl-1-thio-β-D-galactopyranoside and incubation continued for 4 h. The cells were harvested and resuspended in 10 mL of lysis buffer [20 mM Tris, pH 7.4, 1 mM EDTA, 4 μg/mL pepstatin A, 4 μg/mL aprotinin, 0.1 M PMSF (phenylmethylsulfonyl fluoride)]. After 3 freeze−thaw cycles, 800 units of DNase (Sigma), 5 units of RNase (Sigma), and 10 mM $MgCl_2$ were added to the cell lysate, and incubation was carried out at room temperature on the nutator for 2 h with subsequent centrifugation at 28000*g* for 45 min. The protein was filtered through a 0.2 μm filter and loaded onto a Sephacryl S-300HR molecular sieve column (120 × 2.6 cm). SDS−PAGE was used to examine the fractions; those containing the wild-type and mutant αA-crystallins were pooled and concentrated by ultrafiltration in an Amicon stirred cell.

SDS−PAGE and Western Blot. SDS−PAGE was performed using a 12% separating gel and a 4% stacking gel under reducing conditions, according to the method of Laemmli (*31*). Three micrograms was run at 200 V for 45 min, and the proteins were then blotted onto a Millipore poly(vinylidene difluoride) (PVDF) membrane. Rabbit anti-αA/αB-crystallin peptide polyclonal antibody (Stress Gene) was used as the first antibody, and the crystallins were visualized by incubating with Western Blue stabilized substrate for alkaline phosphatase (Protoblot System, Promega).

Size-Exclusion Chromatography for Determining Molecular Masses. The aggregate sizes were determined by size-exclusion chromatography performed with a water-jacketed Sephacryl-S-300 HR column (1.6 × 100 cm) at different temperatures (25, 37, and 45 °C). A constant flow-rate (34 mL/h) and temperatures were maintained by a peristaltic pump and water bath, respectively. Protein, 2 mg in 1 mL of PBS buffer, pH 7.4, was incubated for 1 h at the above temperatures and then applied to the column which had been equilibrated to the desired temperatures. The elution was performed with the same buffer, and fractions of 1 mL each were collected and monitored at 280 nm. High molecular mass standards (Sigma) were used to calibrate the column. Molecular masses (M) were determined from a plot of log M vs V_e/V_o (V_e = elution volume and V_o = void volume).

Circular Dichroism Measurements. To investigate secondary and tertiary structural changes of recombinant rat αA-wild-type, αA-S142C, and αA-R116C, their near- and far-UV CD spectra were recorded at 25 and 37 °C using a Jasco 710 spectropolarimeter. Protein concentrations of 0.5 and 0.1 mg/mL in 50 mM potassium phosphate buffer, pH 7.4, were used for recording the near- and far-UV CD spectra, respectively. The reported CD spectra are the average of five scans smoothed. Secondary structure parameters were estimated by the computer program PROSEC derived from Yang et al. (*32*).

Determination of Molecular Chaperone-like Activity of αA-Crystallin. The aggregation and denaturation of insulin or alcohol dehydrogenase (ADH) in the absence and in the presence of recombinant wild-type and mutant αA-crystallins was measured in a Shimadzu UV160 spectrophotometer equipped with a temperature-regulated cell holder. Ratios of 1:1 and 2:1 αA-crystallin to insulin and αA-crystallin to ADH were used to determine chaperone-like activity. Insulin was denatured using 20 mM DTT and ADH using 10 mM EDTA at 37 ± 1 °C, and light scattering was monitored at 360 nm.

Determination of Protein Stability of αA-Wild-Type and Its Mutants. The heat stability of 1 mg/mL protein in PBS, pH 7.4, was tested at 25, 37, and 45 °C by monitoring light scattering at 360 nm. Stability studies were also done in the presence of EDTA or DTT.

Tryptophan Fluorescence Measurements. Fluorescence measurements were preformed with a Shimadzu RF-540 spectrofluorophotometer. Protein samples of 0.1 mg/mL in 50 mM phosphate buffer, pH 7.4, were used. Excitation was fixed at 295 nm and emission scanned between 310 and 400 nm.

ANS Fluorescence Measurements. The hydrophobic probe ANS binding studies were done as follows: to 1 mL of protein (0.1 mg/mL) solution in 50 mM phosphate buffer, pH 7.4, was added 10 μL of 20 mM methanolic solution of ANS and incubated for 2 h. Emission spectra were recorded

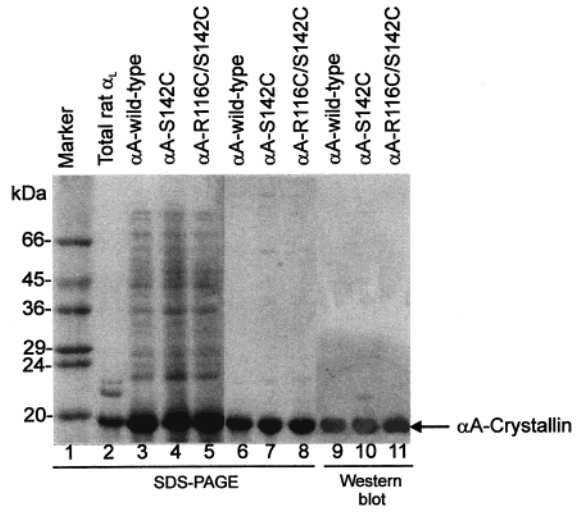

FIGURE 1: SDS−PAGE and Western blot of bacterial expressed rat αA-wild-type and mutants S142C and R116C/S142C. Lane 2: αL fraction from rat lens. Lanes 3−5: total cell lysate of expessed αA-crystallins. Lanes 6−8: size exclusion chromatograpy purified αA-crystallins. Lanes 9−11: Western blot of lanes 6−8 with anti-αA/αB polyclonal antibody.

between 420 and 600 nm while the excitation wavelength was fixed at 390 nm.

RESULTS

Cloning, Mutagenesis, Expression, and Purification of Wild-Type and Mutant Rat αA-Crystallins. The rat αA-crystallin DNA obtained by RT-PCR was cloned into the expression vector pET-23d(+). The nucleotide sequence was confirmed by automated sequencing and found to be identical to the coding region of GenBank sequence accession number U47922. Rat αA-crystallin has only one cysteine (position 131) whereas human αA-crystallin has two cysteines (positions 131 and 142). Therefore, a cysteine was introduced at position 142 (S142C) in the rat αA-crystallin in order to mimic the number of cysteines in the native human αA-crystallin. Then, using the αA-S142C mutant amplicon as the template, a second mutant, R116C/S142C (R116C), was generated. This mutant is structurally similar to the genetic variant previously reported to have caused congenital cataract in humans (*30*). The expression host BL21(DE3)pLysS *E. coli* cells were transformed with pET-23d(+)-αA amplicons. After induction with IPTG and further growth, the cells were pelleted and lysed, and protein was analyzed by SDS−PAGE (Figure 1 , lanes 3−5). The recombinant αA-crystallins and the αA-crystallin from the total rat α_L-crystallin fraction corresponded approximately to the 20 kDa band of the marker. The expressed proteins were purified by Sephacryl gel permeation chromatography, which resulted in about 95% pure recombinant αA-crystallin (Figure 1, lanes 6−8). During purification, it was noticed that the αA-R116C mutant eluted ahead of the wild-type and the αA-S142C mutant, indicating that αA-R116C was more oligomerized than the others. After purification, Western blotting with a rabbit anti-αA/αB-crystallin peptide polyclonal antibody further confirmed the identity of the recombinant αA-crystallin (Figure 1, lanes 9−11).

Molecular Masses of the Recombinant Wild-Type and Mutant αA-Crystallins. To ascertain if mutation of Arg-116 to Cys influenced αA-crystallin oligomerization, size-exclusion chromatography was performed after protein purification. αA-Wild-type, αA-S142C, and αA-R116C were analyzed at 25, 37, and 45 °C; representative chromatograms are given in Figure 2 and their molecular masses are given in Table 1. At 25 °C, the size of the R116C mutant was close to 2000 kDa whereas for the wild-type and the S142C mutant the values were 581 and 528 kDa, respectively. At 37 and 45 °C, the size of the R116C mutant decreased to about 1400 and 900 kDa, respectively, while the size of the wild-type and S142C remained nearly the same.

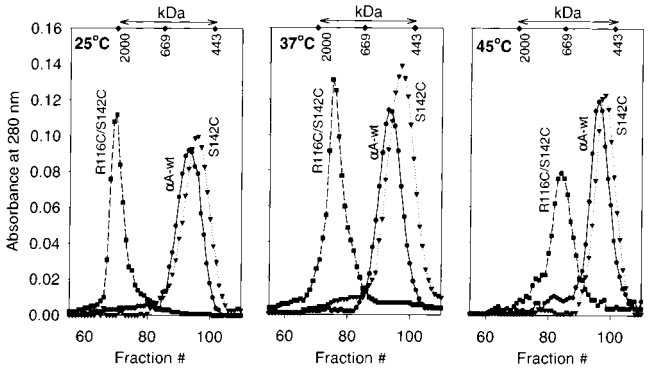

FIGURE 2: Determination of the oligomeric sizes of recombinant αA-crystallins by size exclusion chromatography with a temperature-regulated Sephacryl S-300 HR column at 25, 37, and 45 °C. The numbers on the top refer to the masses of the molecular weight protein standards.

Table 1: Molecular Masses[a] (kDa) vs αA-Wild-Type (αA-WT) and Its Mutants

temp (°C)	αA-WT	αA-S142C	αA-R116C
25	581	528	2000
37	581	489	1403
45	516	477	903

[a] Molecular masses (M) were determined from a plot of log M vs V_e/V_o of molecular mass standards.

Conformational Studies. The far-UV and near-UV CD spectra of rat αA-wild-type and S142C and R116C mutants, recorded at 25 and 37 °C, are shown in Figure 3. The far-UV profiles indicate the minima to be around 217 nm, which is the characteristic of mainly β-conformation even though their mean residue ellipticity values have been found to be slightly different (Figure 3A,B). Estimates of the secondary structure parameters were done by the computer program PROSEC. At 25 °C, contents of α-helix, β-sheet, β-turn, and random coil for αA-wild-type were 9.3, 44.1, 21.4, and 22.2%, respectively; similar levels of the various structural components were found in the two mutants. These data are in good agreement with the published values for αA-crystallin (*33*). However, at 37 °C, the data differ markedly. While the α-helix conformation remained the same, the β-sheet content was reduced by 50% with concomitant increase in random coil conformation. Near-UV CD spectra of αA-wild-type, S142C mutant, and R116C mutant (Figure 3C,D) show the maxima at 259 and 265 nm, which are the characteristics of phenylalanine fine structure. The remaining transitions between 270 and 290 nm arise from Tyr and/or Trp residues. The negative vibronic transition at around 293 nm is considered to be due to the contribution of Trp residues. But, for αA-R116C there are no distinct bonds due to Tyr and/or Trp. This indicates different Tyr and Trp microenvironments in this mutant when compared with αA-

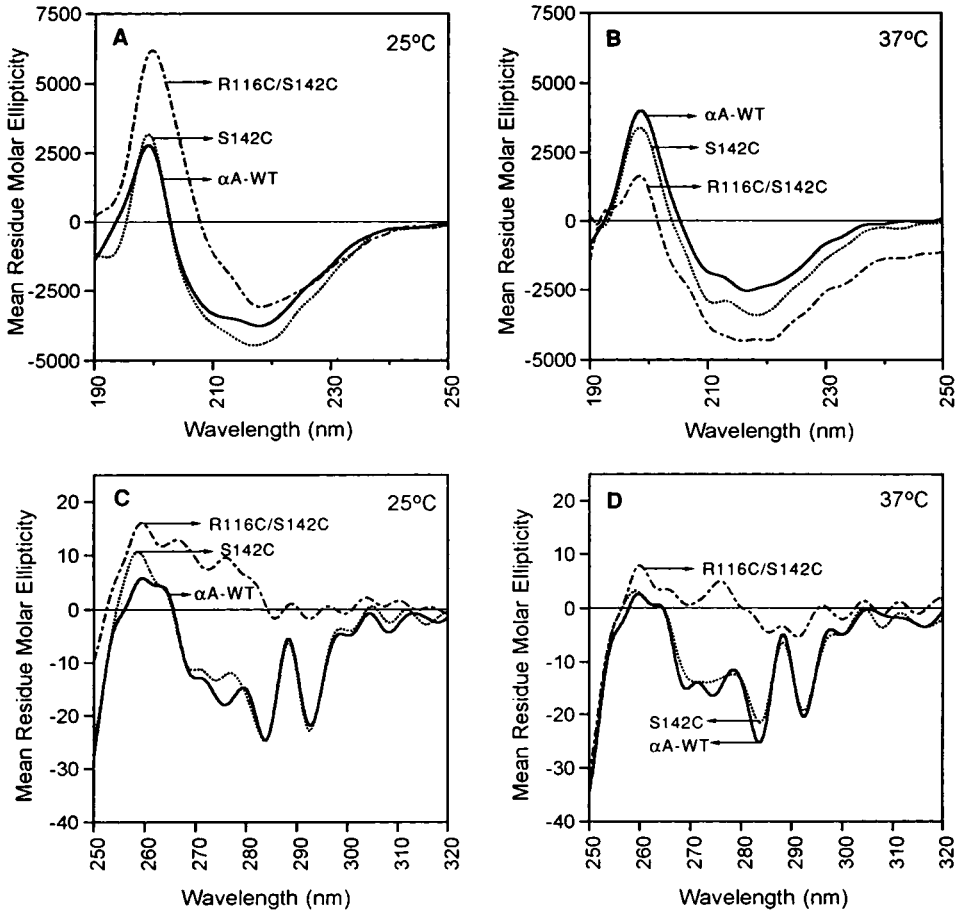

FIGURE 3: Far-UV CD spectra for αA-wild-type and S142C and R116C/S142C mutants at (A) 25 °C and (B) 37 °C. Near-UV spectra for these αA-crystallins at (C) 25 °C and (D) 37 °C. The protein concentrations for far-UV CD and near-UV CD measurements were 0.1 and 0.5 mg/mL, respectively.

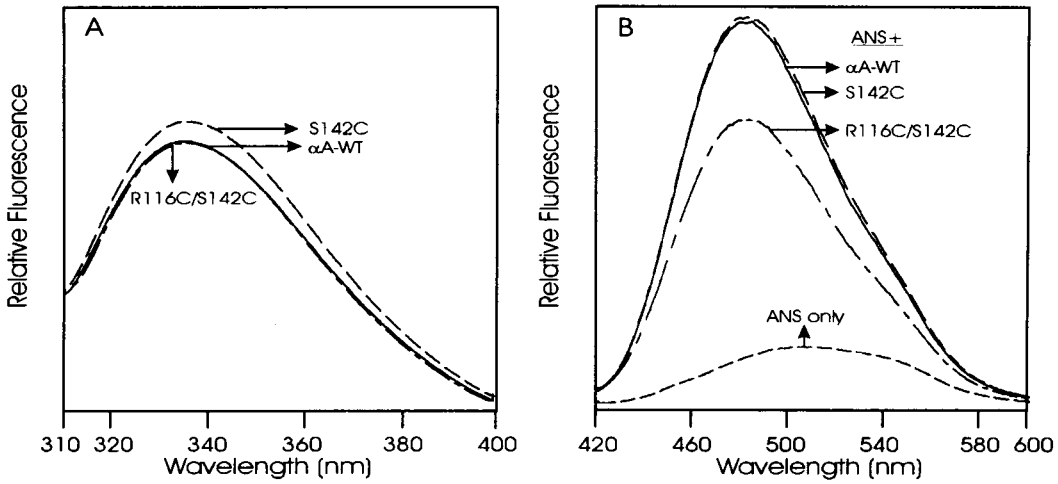

FIGURE 4: Trp fluorescence spectra (A) and ANS fluorescence spectra (B) for αA-wild-type and S142C and R116C/S142C mutants at 37 °C. For Trp fluorescence measurements, the excitation wavelength was 295 nm, and for ANS fluorescence, 390 nm and the protein concentration was 0.1 mg/mL.

wild-type and αA-S142C. Figure 4 represents fluorescence monitoring before and after ANS binding. Intrinsic Trp fluorescence spectra showed similar wavelength maxima and fluorescence intensity at around 336 nm for all three αA-crystallins (Figure 4A). ANS fluoresces at about 512 nm, and in the presence of α-crystallin, it fluoresces significantly intense and blue-shifts to 483 nm (Figure 4B). ANS binding to the R116C mutant was decreased significantly, implying that the available hydrophobic surface is decreased appreciably.

Molecular Chaperone-like Activity of the Wild-Type and the Mutant S142C and R116C αA-Crystallins. Chaperone-like activity was measured at 37 °C by in vitro assays using insulin and ADH as target proteins with two different proportions of αA:target protein (1:1 and 2:1). Different preparations of the αA-wild-type, mutant αA-S142C, and

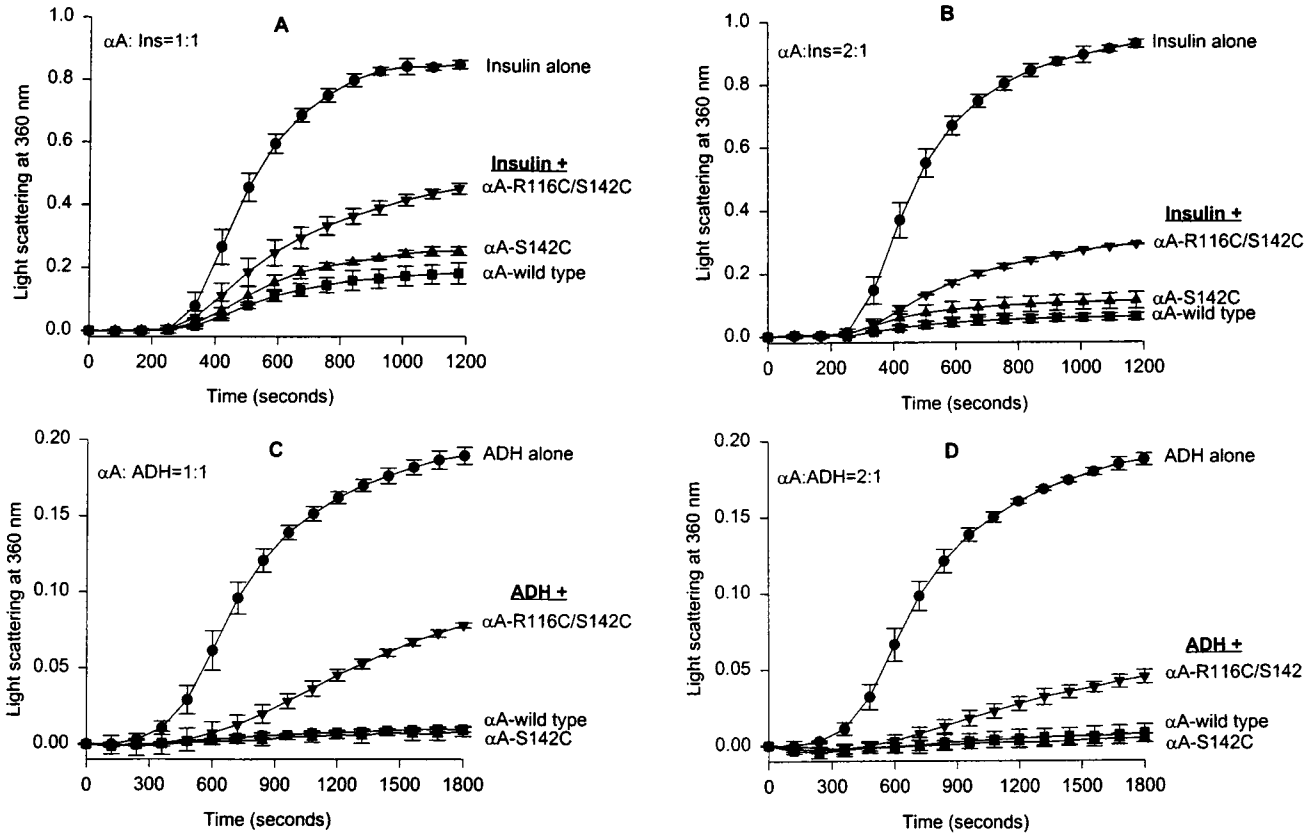

FIGURE 5: Chaperone-like activity of αA-wild-type and S142C and R116C/S142C mutants at 37 °C using insulin as the target protein in the presence of DTT (A, B) and ADH as the target protein in the presence of EDTA (C, D). Each curve is the mean of chaperone assays done on three different preparations, and bars represent standard deviations.

mutant αA-R116C were assayed, and the means ± SD of protein denaturation curves are presented (Figure 5). In the absence of αA-crystallin, insulin is fully aggregated by DTT at 37 °C whereas the presence of αA-crystallin prevents this aggregation (Figure 5A,B). This inhibitory effect on insulin aggregation is taken as the chaperone-like activity (chaperone activity or chaperone function). The chaperone activity of αA-S142C was not significantly different from αA-wild-type. αA-R116C, on the other hand, showed about 40% loss in chaperone activity when the α-crystallin-to-insulin ratio was 1:1 (Figure 5A). A similar, but slightly smaller, decrease of chaperone activity was observed at a α:insulin ratio of 2:1 (Figure 5B). ADH was used as a target protein in the presence of EDTA with no DTT. Chaperone activity assays were done with ADH as the target protein, which gave similar results (Figure 5C,D).

Heat Stability of the Wild-Type and Mutant αA-Crystallins. Heat stability of the wild-type and the R116C and S142C mutants was determined at 25, 37, and 45 °C by monitoring light scattering at these temperatures using the same setup as in chaperone assays in the absence of any target proteins; the data are presented in Figure 6. It is well-known that the aborbance at 360 nm is due to light scattering of the protein molecule which is directly proportional to the size. As expected, the R116C mutant gave higher absorbance than the wild-type and the S142C mutant. At all three temperatures, the wild-type and the S142C mutant showed no evidence of denaturation and aggregation to molecules or disaggregation to smaller size. The R116C mutant, on the other hand, behaved very differently at 37 and 45 °C; at these temperatures, light scattering significantly decreased, indicating dissociation of the protein into smaller molecules. This observation corroborates with our size exclusion chromatography experiments which also showed dissociation of the R116C super-oligomers into smaller molecules at 37 and 45 °C. The presence of DTT or EDTA did not show any additional effect on the protein stability at all temperatures.

DISCUSSION

Autosomal dominant congenital cataracts are the major form of familial cataract. Mutations in mammalian crystallin genes associated with hereditary cataracts have been reported in human and other species (*23*−*30*). The basis for the present study is a recent report by Litt et al. (*30*) of autosomal dominant congenital cataract in human associated with a missense mutation, R116C, in αA-crystallin. These authors have speculated that the mutant αA-polypeptide might have an increased tendency to aggregate because of its decreased positive charge and this may result in the loss of chaperone activity. We investigated this possibility by generating a rat αA-crystallin with strong structural similarity to the above mutant. In fact, three different recombinant rat αA-crystallins were generated: αA-wild-type, mutant αA-S142C (structurally similar to normal human αA-crystallin), and mutant αA-R116C (structurally similar to the genetic variant causing cataract). By utilizing these αA-crystallins, we were able to conclude that the variant αA-R116C forms a highly oligomerized protein (Figure 2) with modified structure (Figures 3 and 4) and partially impaired chaperone function (Figure 5). It is also noteworthy that the dynamic quaternary structure of the R116C mutant is temperature-dependent (Figure 6);

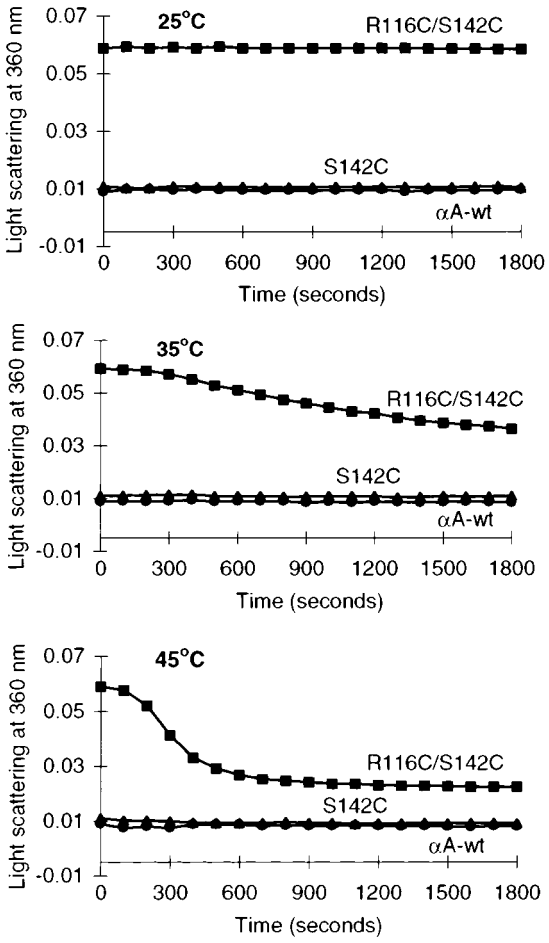

FIGURE 6: Heat stability curves of αA-wild-type and S142C and R116C/S142C mutants at 25, 37, and 45 °C without the target protein. Light scattering was recorded at 360 nm.

at physiological temperature, it has more than twice the size of αA-wild-type.

The mutant αA-R116C had an oligomeric size 2−4 times larger (depending on the temperature) than either the αA-wild-type or the αA-S142C (Figure 2). Proper protein assembly may depend on a salt bridge involving the positively charged guanidino group of Arg-116, the absence of which probably explains increased oligomeric size. αA-R116C, which is conserved in many species, lies in a buried region of the protein (*21*). Arginines in general are known to be involved in salt bridges and hydrogen bonds. Before the discovery of the autosomal dominant congenital cataract associated with a R116C mutation in αA-crystallin, Berengian et al. (*21*) made a series of cysteine mutants extending between amino acid residues 109 and 120 in rat αA-crystallin. The purpose of their study was to apply site-directed spin-labeling in the form of attached nitroxides to investigate the role of the above sequence in the assembly of αA-crystallin quaternary structure. Unlike the mutants used in the present study, they mutated Cys-131 to Ala and did not mutate Ser-142 to Cys. The mutant R116C with a nitroxide attached to the Cys studied by these investigators had a molecular mass 30% higher and chaperone activity similar to the wild-type αA-crystallin. This contradicts our observation, probably because the mutant characterized by the above authors has the mutated cysteine carrying a nitroxide and this additional derivatization seems to suppress excessive protein aggregation. Moreover, the rat αA-crystallin R116C mutant used in our study has cysteines in two other positions, namely, 131 and 142, similar to the human αA-crystallin. Since there are a total of three Cys in R116C, it is possible that aggregation of the R116C mutant involves inter- or intrapolypeptide disulfides. However, the oligomeric sizes and chaperone activity were not influenced by DTT treatment (Figures 2 and 5), indicating that protein disulfides are not formed, or, if formed, do not affect oligomerization and chaperone function.

There is strong evidence that mutation of Arg-116 to Cys causes conformational changes in the αA-crystallin (Figures 3 and 4). Since chaperone assays were done at 37 °C, we performed all the biophysical studies at 25 and 37 °C. CD studies clearly showed structural and conformational differences at 37 °C, in particular. Although intrinsic tryptophan fluorescence spectra (Figure 4A) did not suggest the presence of any significant conformational changes, near-UV CD spectra implicated changes in Trp and Tyr microenvironments. Near-UV CD spectra are sensitive to changes in the fine structure and microenvironment of Trp and Tyr. Interestingly, ANS binding showed significantly reduced surface hydrophobicity in the R116C mutant (Figure 4B). In fact, hydrophobic surfaces are believed to be needed for proper chaperoning function, and their loss is expected to reduce chaperone-like function. However, mutation of R116C by itself is not expected to decrease the availability of hydrophobic surfaces unless it causes changes in protein conformation.

Another most noteworthy example of a single point mutation in one of the α-crystallin subunits is the missense mutation R120G in αB-crystallin which has been shown to cosegregate with a desmin-related myopathy in a French family (*34*). This mutant αB-crystallin has been characterized recently by Bova et al. (*35*), who showed irregular quaternary structure and complete loss of chaperone function. Interestingly, Arg-120, in αB-crystallin, lies in the most conserved region of the small hsp family (*36*). It is noteworthy that the oligomeric size of this mutant was nearly 1400 kDa. Arg-116 of αA-crystallin also lies in a conserved region of residues 109 through 120 (*21*)and was shown to exist in a buried environment with no access to aqueous solvent (*21*). Buried charged amino acids are believed to form salt bridges with residues of opposite charges, and the absence of such salt bridges could lead to protein conformational changes. The site-directed D69S mutant of αA-crystallin resulted in reduced chaperone-like function (*37*). Thus, it appears that α-crystallin may not withstand mutation of a charged residue like Arg to an uncharged residue, within a conserved region, in particular.

To assess the chaperone-like activity at physiological temperature, we have used two independent assay systems with insulin and ADH as target proteins. Both systems showed about 40% loss in chaperone activity when the αA:target protein proportion (w/w) was 1:1 (Figure 5). The physiological significance of this finding comes from the fact that significant loss of chaperone activity was seen when the α-crystallin proportion in the assay system was similar to the proportion in human lenses. It is also noteworthy that loss in chaperone activity, although smaller (21−27%), could be demonstrated even when αA:target protein proportion was raised to 2:1, which is significantly higher than in human lens. It was crucial that we performed all the biophysical

studies at 37 °C to relate structural changes to a decrease in function at this temperature. Structural and conformational changes are present in the R116C mutant at 37 °C (Figures 3 and 4), although the oligomeric size is smaller at 37 °C than at 25 °C due to some dissociation of the super-oligomers. From the present study, it appears that the molecular basis for the development of congenital cataract in the affected individuals is the formation of highly oligomerized αA-crystallin with structural and conformational changes and defective chaperone-like function. However, it can be argued that, since αB-crystallin is a better chaperone than αA-crystallin, the loss of chaperone activity of the R116C mutant may play only a small role in cataractogenesis. On the other hand, it is known that this cataract develops mostly in infancy and late childhood (*30*) and the proportion of αA-R116C:αB would be 2:1 in these patients (*38*). So, it is conceivable that 40% loss in chaperone activity contributes to cataractogenesis.

ACKNOWLEDGMENT

We thank Prof. Leon Dure and Ms. Tracy Grant of the University of Georgia for assistance in CD measurements.

REFERENCES

1. van der Ouderaa, F. J., de Jong, W. W., Hilderink, A., and Bloemendal, H. (1973) *Eur. J. Biochem. 39*, 207−222.
2. van der Ouderaa, F. J., de Jong, W. W., and Bloemendal, H. (1974) *Eur. J. Biochem. 49*, 157−168.
3. Hawkins, J. W., van Keuren, M. L., Piatigorsky, J., Law, M. L., Patterson, D., and Kao, F. T. (1987) *Hum. Genet. 76*, 375−380.
4. Ngo, J. T., Klisak, I., Dubin, R. A., Piatigorsky, J., Mohandas, T., Sparkes, R. S., and Bateman, J. B. (1989) *Genomics 5*, 665−669.
5. Deretic, D., Aebersold, R. H., Morrison, H. D., and Papenmaster, D. S. (1994) *J. Biol Chem. 269*, 16853−16861.
6. Srinivasan, A. N., Nagineni, C. N., and Bhat, S. P. (1992) *J. Biol. Chem. 267*, 23337−23341.
7. Bhat, S. P., and Nagineni, C. N. (1989) *Biochem. Biophys. Res. Commun. 158*, 319−325.
8. Dubin, R. A., Wawrousek, E. F., and Piatigorsky, J. (1989) *Mol. Cell. Biol. 9*, 1083−1091.
9. Lowe, J., McDermot, H., Pike, I., Spendlove, I., Landon, M., and Mayer, R. J. (1992) *J. Pathol. 166*, 61−68.
10. Iwaki, T., Wisniewski, T., Iwaki, A., Corbin, E., Tomokane, N., Tateishi, J., and Goldman, J. E. (1992) *Am. J. Pathol. 140*, 345−356.
11. Scotting, P., McDermott, H., and Mayer, R. J. (1991) *FEBS Lett. 285*, 75−79.
12. Iwaki, T., Iwaki, A., Liem, R. K., and Goldman, J. E. (1991) *Kidney Int. 40*, 52−56.
13. Renkawek, K., Bosman, G. J., and de Jong, W. W. (1994) *Acta Neuropathol. 87*, 155−160.
14. Harding, J. J., and Crabbe, M. J. C. (1984) The Lens: development, protein, metabolism and cataract. in *The Eye*, pp 207−492, Academic Press, New York.
15. Augusteyn, R. C., Parkhill, E. M., and Stevens, A. (1992) *Exp. Eye Res. 54*, 219−228.
16. Ingolia, T. D., and Craig, E. A. (1982) *Proc. Natl. Acad. Sci. U.S.A. 79*, 2360−2364.
17. Horwitz, J. (1992) *Proc. Natl. Acad. Sci. U.S.A. 89*, 10449−10453.
18. Brady, J. P., Garland, D., Duglas-Tabor, Y., Robison, W. G., Groome, A., and Wawrousek, E. F. (1997) *Proc. Natl. Acad. Sci. U.S.A. 94*, 884−889.
19. Haley, D. A., Horwitz, J., and Stewart, P. L. (1998) *Invest. Ophthalmol. Visual Sci. 39*, S870.
20. Kim, K. K., Kim, R., and Kim, S. (1998) *Nature 394*, 595−599.
21. Berengian, A. R., Bova, M. P., and Mchaourab, H. S. (1997) *Biochemistry 36*, 9951−9957.
22. Koteiche, H. A., Berengian, A. R., and Mchaourab, H. S. (1998) *Biochemistry 37*, 12681−12688.
23. Lund, A. M., Eiberg, H., Rosenberg, T., and Warburg, M. (1992) *Clin. Genet. 41*, 65−69.
24. Reese, P., Truck-Mullerr, C., and Maumenee, I. (1987) *Arch. Opthalmol. 105*, 1382−1384.
25. Rodriguez, I. R., Gonzalez, P., Zigler, J. S., Jr., and Borras, T. (1992) *Biochim. Biophys. Acta 1180*, 44−52.
26. Cartier, M., Breitman, M. L., and Tsui, L. C. (1992) *Nat. Genet. 2*, 42−45.
27. Chambers, C., and Russell, P. (1991) *J. Biol. Chem. 266*, 6742−6746.
28. Litt, M., Carrero-Valenzuela, R., LaMorticella, D. M., Schultz, D. W., Mitchell, T. N., Kramer, P., and Maumenee, I. H. (1997) *Hum. Mol. Genet. 6*, 665−668.
29. Brakenhoff, R. H., Henskens, H. A., van Rossum, M. W., Lubsen, N. H., and Schoenmakers, J. G. (1994) *Hum. Mol. Genet. 3*, 279−283.
30. Litt, M., Kramer, P., LaMorticella, D. M., Murphey, W., Lovrien, E. W., and Weleber, R. G. (1998) *Hum. Mol. Genet. 7*, 471−474.
31. Laemmli, U. K. (1970) *Nature 227*, 680−685.
32. Yang, J. T., Wu, C. H. C., and Martinez, H. M. (1986) *Methods Enzymol. 130*, 208−269.
33. Sun, T., Das, B. K., and Liang, J. N. (1997) *J. Biol. Chem. 272*, 6220−6225.
34. Vicart, P., Caurn, A., Guicheney, P., Li, A., Prevost, M. C., Faure, A., Chateau, D., Chapou, F., Tone, F., Dupret, J. M., Paulin, D., and Fardeau, M. (1998) *Nat. Genet. 20*, 92−95.
35. Bova, M. P., Yaron, O., Huang, Q., Ding, L., Haley, D., Stewart, P., and Horwitz, J. (1999) *Proc. Natl. Acad. Sci. U.S.A. 96*, 6137−6142.
36. de Jong, W. W., Leurissen, J. A. M., and Voorter, C. E. M. (1993) *Mol. Biol. Evol. 10*, 103−126.
37. Smulders, R. H. P. H., Merck, K. B., Aendekerk, J., Horwitz, J., Takemoto, L., Slingsby, C., Bloemendal, H., and de Jong, W. W. (1995) *Eur. J. Biochem. 232*, 834−838.
38. Swamy, M. S., and Abraham, E. C. (1991) *Curr. Eye Res. 10*, 213−220.

BI991656B